

NTM Seed Island Formation by Error Field in Rotating Plasma

N.V. Ivanov, A.N. Chudnovskiy, A.M. Kakurin, I.I. Orlovskiy

Nuclear Fusion Institute, RRC «Kurchatov Institute», Moscow, Russia

Introduction

The dependence of the $m = 2$ mode rotation irregularity [1-4] on the mode amplitude in the presence of the Error Field (see [5, 6]) in T-10 tokamak is considered. The rotation irregularity is observed as a dependence of the mode angular velocity on the mode instantaneous angular position. Since the angular position of the rotating magnetic island changes cyclically, the angular velocity of the mode rotation goes through cyclical variations as well. Under the appropriate variation of plasma conditions, the increase of the rotation irregularity is ultimately followed by the termination of the mode rotation (i.e. mode locking).

The experimental data are simulated with the TEAR code [4, 9, 10] utilizing a model for the non-linear Rutherford tearing mode [7, 8] in the presence of plasma rotation and an External Helical Magnetic Perturbation (EHMP), which simulates the Error Field. The rotation velocity of the mode is represented by a superposition of the plasma rotation velocity affected by the plasma interaction with the EHMP and the velocity of the mode with respect to the plasma that arises as a characteristic of an externally driven non-linear tearing mode. The results are analysed from the point of view of the NTM seed island formation by the Error Field in rotating plasma.

Experimental Arrangement and Processing of the MHD Data

T-10 is a tokamak with a circular plasma cross-section. The major and minor radii of the vacuum vessel are $R = 1.5$ m and $b = 0.42$ m, the radius of the permanent circular limiter is 0.33 m. The experiments were carried out at the discharge parameters: toroidal magnetic field $B_T = 2.4$ T, discharge current $I_p = 240$ kA. The plasma minor radius determined by the position of the movable rail limiter was $a = 0.27$ m. In our experiment the $m = 2$, $n = 1$ harmonic of the Error Field can be estimated as 10^{-4} T at the plasma boundary.

The space structure of the MHD mode is measured with a set of poloidal magnetic field sensors located at the inner side of the vacuum vessel. The experimental MHD signal processing procedure includes a decomposition of the measured magnetic perturbation to a set of spatial Fourier harmonics with different poloidal and toroidal numbers. For each harmonic with certain m and n numbers the poloidal magnetic field perturbation at the radial position of the magnetic sensors is

$B_\theta(\theta, \varphi, t) = B_{\theta C}(t)\cos(m\theta + n\varphi) + B_{\theta S}(t)\sin(m\theta + n\varphi)$, where φ and θ are the toroidal and poloidal angles, $B_{\theta C}(t)$ and $B_{\theta S}(t)$ are the cosine and sine components of the measured harmonic of the magnetic perturbation. The space amplitude of the harmonic is

$\text{Ampl } B_\theta(t) = \sqrt{B_{\theta C}^2 + B_{\theta S}^2}$, the space phase of this harmonic is $\Phi(t) = \arctan\left(\frac{B_{\theta S}}{B_{\theta C}}\right)$ and

the instantaneous value of the mode angular frequency is $\Omega(t) = d\Phi/dt$. The mode rotation irregularity is defined as $(\Delta\Omega/2)/\langle\Omega\rangle$ where $\Delta\Omega$ is the difference between maximum and minimum values of Ω over the oscillation period and $\langle\Omega\rangle$ is its average value.

Experimental Observations

The experimental waveforms of the $m = 2$ mode signals during the process of the mode amplitude variation in time are shown in Fig. 1. The mode signals in the time intervals Δt_1 , Δt_2 and Δt_3 for different levels of the mode amplitude are shown in Fig. 2 together with the waveform of the mode frequency. The dependence of the mode rotation irregularity on the mode amplitude is plotted in Fig. 3. In Fig. 2 and Fig. 3, one can see that along with the mode amplitude variation, the rotation irregularity increases in both cases of sufficiently big and small amplitudes.

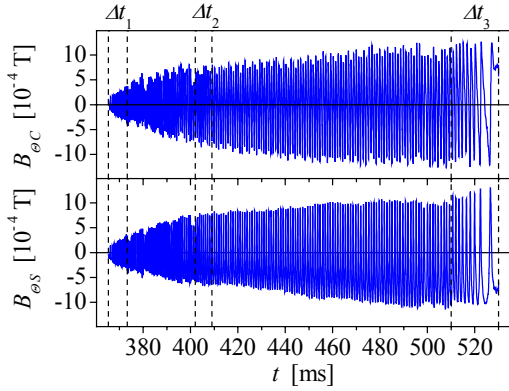


Fig. 1. Waveforms of the $m = 2$ mode cosine, $B_{\theta C}$, and sine, $B_{\theta S}$, space components. The time intervals Δt_1 , Δt_2 and Δt_3 are shown with vertical dashed lines

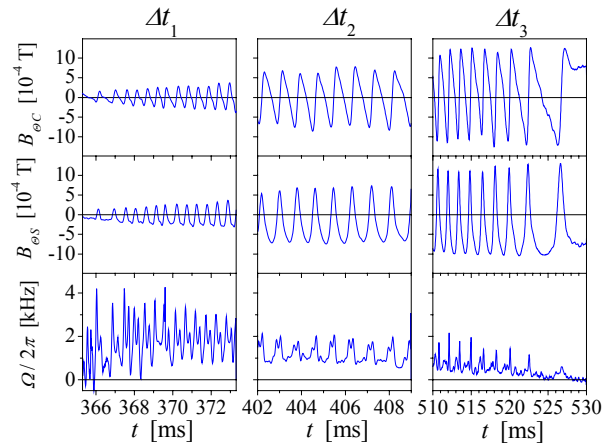


Fig. 2. Waveforms of the $m = 2$ mode cosine, $B_{\theta C}$, sine, $B_{\theta S}$, space components and the instantaneous value of the mode frequency, Ω , in the time intervals Δt_1 , Δt_2 and Δt_3

Numerical Modelling

In the TEAR code (see [4, 9, 10]), the non-linear tearing mode rotation in presence of the EHMP of the same poloidal and toroidal numbers is simulated in cylindrical approximation using the Rutherford model [7, 8]. In this paper, we assume that the EHMP is produced by a current layer at the radius $r = r_i$ outside the plasma. The equations

$$\frac{\partial}{\partial r} \left(r \frac{\partial \Psi_{C,S}}{\partial r} \right) - \left(\frac{m^2}{r} + \frac{\mu_0 R}{B_r} \frac{\partial j / \partial r}{\mu(r) - n/m} \right) \Psi_{C,S} + \mu_0 r i_{C,S} \delta(r - r_i) = 0 \quad (1), (2)$$

are used for the calculation of the radial distribution of the cosine, Ψ_C , and sine, Ψ_S , components of the perturbed helical flux function $\Psi = \Psi_C(r, t) \cos(m\theta + n\varphi) + \Psi_S(r, t) \sin(m\theta + n\varphi)$, satisfying the boundary conditions $\Psi_{C,S}(0) = \Psi_{C,S}(\infty) = 0$. The perturbed poloidal and radial components of magnetic field are given by $B_\theta = -\partial \Psi / \partial r$ and $B_r = (1/r) \partial \Psi / \partial \theta$. In (1) and (2), $j(r)$ is the plasma current density, $\mu(r) = 1/q(r)$, $\mu_0 = 4\pi \times 10^{-7} \text{ Hm}^{-1}$, i_C and i_S are the cosine and sine components of the external helical current surface density at the radius $r = r_i$: $i = i_C(t) \cos(m\theta + n\varphi) + i_S(t) \sin(m\theta + n\varphi)$ which produces the EHMP. The time evolution of the cosine and sine components of the magnetic flux perturbation at $r = r_S$, where $\mu(r_S) = n/m$, is described by the equations:

$$\frac{d\Psi_C}{dt} = \pi a^2 \omega_R \frac{\Delta'_C(W)}{W} \Psi_C - \Omega_r \Psi_S, \quad (3)$$

$$\frac{d\Psi_S}{dt} = \pi a^2 \omega_R \frac{\Delta'_S(W)}{W} \Psi_S + \Omega_r \Psi_C. \quad (4)$$

In (3) and (4), $\omega_R = 1/\tau_R$, $\tau_R = \mu_0 a^2/\eta$ is the resistive time. The right-hand sides of the equations (3) and (4) include stability parameters for the cosine and sine components of the magnetic flux perturbation:

$$\Delta'_{C,S} = \frac{\Psi'_{C,S}(r_S + W/2) - \Psi'_{C,S}(r_S - W/2)}{\Psi_{C,S}(r_S)}, \text{ where } W = 4 \sqrt{\frac{R \sqrt{\Psi_C^2 + \Psi_S^2}}{r_S B_T |d\mu/dr|}}_{r_S} \text{ is the width of the}$$

magnetic island. In (3) and (4),

$$\Omega_{rl} = mV_\theta/r_S + nV_\phi/R \quad (5)$$

is a parameter depending on the toroidal, V_ϕ , and poloidal, V_θ , rotation velocities of the resonant plasma layer $r_S - W/2 \leq r \leq r_S + W/2$. Similar to [11-13], we use the equations of angular motion in the toroidal and poloidal directions to calculate the time variations of V_ϕ , and V_θ . We assume that the plasma inertial torque is balanced by the sum of the electromagnetic, $M_{EM \phi, \theta}$, and viscous, $M_{V \phi, \theta}$, torques:

$$\frac{I_\phi}{R} \frac{dV_\phi}{dt} = M_{EM \phi} - M_{V \phi} - \frac{V_\phi - V_{0\phi}}{R} \frac{dI_\phi}{dt}, \quad (6)$$

$$\frac{I_\theta}{r_S} \frac{dV_\theta}{dt} = M_{EM \theta} - M_{V \theta} - \frac{V_\theta - V_{0\theta}}{r_S} \frac{dI_\theta}{dt}. \quad (7)$$

In the equations (6) and (7), I_ϕ and I_θ are the toroidal and poloidal moments of inertia of the resonant plasma layer, $V_{0\phi, \theta}$ are the components of the plasma intrinsic rotation velocity outside the resonant plasma layer.

The mode rotation is described by two sets of equations (3), (4) and (6), (7) coupled by (5).

The instantaneous value of the mode frequency is calculated as $\Omega(t) = \frac{d}{dt} \left[\arctan \left(\frac{\Psi_S}{\Psi_C} \right) \right]$.

The tearing mode rotation irregularity is attributed to both the effect on the resonant plasma layer rotation and the effect on the mode rotation with respect to plasma. The resonant plasma layer rotation irregularity is described by (6), (7). This irregularity arises due to the dependences of the electromagnetic torques on the angular shift between the mode and the EHMP. The resonant plasma layer rotation irregularity should increase with the growth of the mode amplitude because the electromagnetic torque is proportional to the mode amplitude.

The mode rotation with respect to plasma is described by (3) and (4). These equations can be considered as the equations for an externally driven non-linear oscillator with the natural frequency Ω_{rl} . The oscillator non-linearity is described by the dependences of $\Delta'_{C,S}$ on W . The external driving force is expressed by the $\Delta'_{C,S}$ dependences on the EHMP. The $\Delta'_{C,S}$ values depend on the shift between the mode angular position and the angular position of

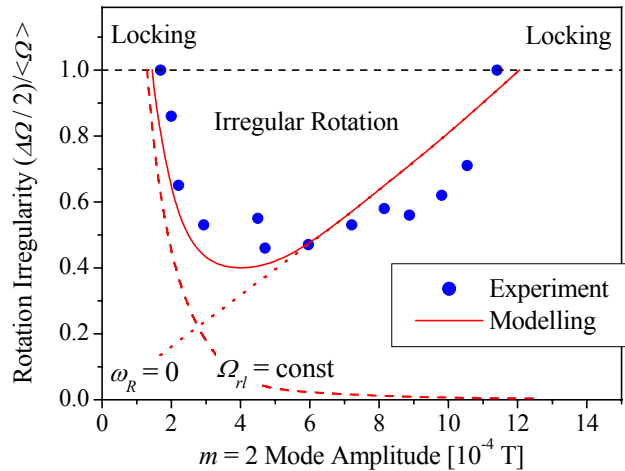


Fig. 3. The dependence of the $m = 2$ mode rotation irregularity on the mode amplitude

the EHMP. The mode rotation irregularity attributed to the mode rotation with respect to the resonant plasma layer should increase with the decrease of the mode amplitude because the slopes of the $\Delta'_{C,S}$ dependences on the EHMP grow with the decrease of $\Psi_{C,S}(r_S)$.

The result of the simulation is shown in Fig.3 for the comparison with the experimental data. Similar to the experiment, the rotation irregularity depends on the mode amplitude. In the case of large magnetic islands, the rotation irregularity and locking take place due to the variations of the resonant plasma layer rotation velocity under influence of the EHMP. In the case of small islands, similar effects on the mode rotation are attributed to the variations of the mode velocity with respect to the resonant plasma layer that arise as a characteristic of the externally driven non-linear tearing mode.

NTM Seed Islands

Coming to the question on the NTM seed islands, we use the TEAR code validated on the T-10 experimental data. We simulate the generation of the magnetic islands in rotating plasma by a permanent Error Field in the case of the originally stable tearing mode, i.e. the case of negative values of $\Delta'(i=0)$. According to the result of this simulation shown in

Fig. 4, the plasma rotation does not prevent the generation a magnetic island locked by the Error Field. The island width weakly depend on the plasma rotation velocity especially for high negative values of $\Delta'(i=0)$. It means that a permanent Error Field can be a source of the NTM seed islands in rotating plasma.

Acknowledgements

We thank S.V.Konovalov for helpful discussions. This work is supported by RF Atomic Energy Agency and scientific school NS-1880.2006.2.

References

1. V.V. Volkov, N.V. Ivanov, A.M Kakurin et al. 22nd EPS Conference on Controlled Fusion and Plasma Physics. Bournemouth 1995. Contributed papers III-077.
V.V. Volkov, N.V. Ivanov, A.M Kakurin et al. Plasma Phys. Rep. **21** (1995) 881.
2. D.A. Gates, T.C. Hender. Nucl. Fusion, **36** (1996) 273.
3. W.A. Craven, A.J. Wootton. Nucl. Fusion **38** (1998) 585.
4. N.V. Ivanov, A.M. Kakurin, I.I. Orlovkiy. 32nd EPS Conference on Plasma Physics and Controlled Fusion, Tarragona (2005) P-5.068, <http://eps2005.ciemat.es/papers/start.htm>
5. R.J. Buttery, M. De'Benedetti, T.C. Hender, et al. Nucl. Fusion **40** (2000) 807.
6. Y. Kikuchi, K.H. Finken, M. Jakubowski, et al. PPCF **48** (2006) 169.
7. P.H. Rutherford. Phys. Fluids **16** (1973) 1903.
8. R.B. White, D.A. Monticello, M.N. Rosenbluth, et al. Phys.Fluids **20** (1977) 800.
9. A.N. Chudnovskiy, Yu.V. Gvozdkov, N.V. Ivanov et al. Nucl. Fusion, **43** (2003) 681.
10. A.N. Chudnovskiy, N.V. Ivanov, A.M. Kakurin et al. Nucl. Fusion, **44** (2004) 287.
11. M.F.F. Nave, J.A. Wesson. Nucl. Fusion, **30** (1990) 2575.
12. R. Fitzpatrick. Nucl. Fusion, **33** (1993) 1049.
13. R. Fitzpatrick. Phys. Plasmas, **5** (1998) 3325.

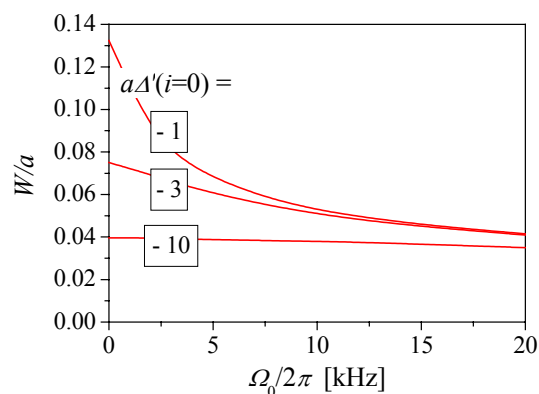


Fig. 4. Dependences of locked-island ($\Omega = 0$) width on $\Omega_0 = mV_{0\theta}/r_S + nV_{0\phi}/R$